In vitro toxicity and photodynamic properties of porphyrinoids bearing imidazolium salts and N-heterocyclic carbene gold(I) complexes

Clémence Rose, Laure Lichon, Morgane Daurat, Sébastien Clément, Magali Gary-Bobo, Sébastien Richeter

INSTITUT DE FRANCE
Académie des sciences

Comptes Rendus

Chimie

Clémence Rose, Laure Lichon, Morgane Daurat, Sébastien Clément, Magali Gary-Bobo and Sébastien Richeter

In vitro toxicity and photodynamic properties of porphyrinoids bearing imidazolium salts and N-heterocyclic carbene gold(I) complexes

Volume 24, Special Issue S3 (2021), p. 83-99

Published online: 17 August 2021
Issue date: 16 December 2021

https://doi.org/10.5802/crchim.98

Part of Special Issue: MAPYRO: the French Fellowship of the Pyrrolic Macrocyclic Ring

Guest editors: Bernard Boitrel (Institut des Sciences Chimiques de Rennes, CNRS-Université de Rennes 1, France) and Jean Weiss (Institut de Chimie de Strasbourg, CNRS-Université de Strasbourg, France)

Les Comptes Rendus. Chimie *sont membres du*
Centre Mersenne pour l'édition scientifique ouverte
www.centre-mersenne.org
e-ISSN : 1878-1543

Comptes Rendus
Chimie
2021, 24, nº S3, p. 83-99
https://doi.org/10.5802/crchim.98

MAPYRO: the French Fellowship of the Pyrrolic Macrocyclic Ring / *MAPYRO: la communauté française des macrocycles pyrroliques*

In vitro toxicity and photodynamic properties of porphyrinoids bearing imidazolium salts and N-heterocyclic carbene gold(I) complexes

Clémence Rose [a], Laure Lichon [b], Morgane Daurat [c], Sébastien Clément [a], Magali Gary-Bobo [b] and Sébastien Richeter [*, a]

[a] ICGM, Univ Montpellier, CNRS, ENSCM, Montpellier, France

[b] IBMM, Univ Montpellier, CNRS, ENSCM, Montpellier, France

[c] NanoMedSyn, 15 avenue Charles Flahault, 34093, Montpellier, France

E-mails: clemence.rose@universite-paris-saclay.fr (C. Rose), laure.lichon@umontpellier.fr (L. Lichon), m.daurat@nanomedsyn.com (M. Daurat), sebastien.clement1@umontpellier.fr (S. Clément), magali.gary-bobo@inserm.fr (M. Gary-Bobo), sebastien.richeter@umontpellier.fr (S. Richeter)

Abstract. Porphyrins bearing imidazolium salts were synthesized and used as N-heterocylic carbene (NHC) precursors for the preparation of gold(I) complexes. The dark toxicity and phototoxicity of the obtained compounds were investigated *in vitro* on MCF-7 breast cancer cells. The obtained data showed that porphyrins equipped with imidazolium salts are non-toxic in the dark and present interesting photodynamic properties. On the contrary, corresponding NHC-gold(I) complexes are not suitable photosensitizers for photodynamic therapy (PDT) applications. Their dark toxicity strongly depends on the nature of the linker between the porphyrin core and the NHC. This work was extended to the synthesis of a pyropheophorbide *a* derivative with a pendant imidazolium group for PDT applications using excitation wavelengths of 450 nm, 545 nm, and importantly of 650 nm.

Keywords. Porphyrinoids, N-heterocyclic carbenes, Gold complexes, Photodynamic therapy, Biocompatibility, Cancer cells.

Available online 17th August 2021

1. Introduction

In the field of cancer therapy, photodynamic therapy (PDT) represents an interesting alternative approach besides chemotherapy, radiotherapy and surgery for some types of cancer, notably skin cancer or tumors accessible to light (directly or thanks to optical fiber) [1–4]. It relies in using a photosensitizer (PS), which is activated by light and able to generate reactive oxygen species (ROS) and singlet oxygen ($^1O_2$). It implies that the PS in its singlet excited state (^{1}PS) can reach its triplet state (^{3}PS) through intersystem crossing (ISC, $^1\text{PS} \rightarrow {}^3\text{PS}$). Then, energy transfer from the ^{3}PS with ground state molecular oxygen in its

* Corresponding author.

triplet state $^3O_2$ leads to the generation of $^1O_2$ (PDT of type 2). Alternatively, electron transfer processes involving the ^{3}PS lead to the formation of ROS and cytotoxic free radicals (PDT of type 1). Ultimately, these strong oxidizing agents may lead to the death of cancer cells through necrotic and apoptotic mechanisms [5–9]. The important aspect of PDT is that only cells containing PS and irradiated with visible light are susceptible to be destroyed. To date, porphyrinoids (including porphyrins, chlorins, phthalocyanines) are among the best performing PS for PDT because of their inherent chemical stability and suitable photophysical properties [10–13]. These tetrapyrrolic aromatic compounds strongly absorb light in the visible region and, more importantly, they are efficient PS to generate $^1O_2$. For example, the $^1O_2$ quantum yield of 5,10,15,20-*meso*-tetraphenylporphyrin (H_2TPP) in toluene is $\Phi_\Delta = 68\%$ [14]. Of course, there are some important drawbacks like their poor water solubility or their lack of selective accumulation in cancer cells, but these drawbacks may be circumvented by appropriate functionalization of the porphyrin core [15–17]. Interestingly, some porphyrins were functionalized with peripheral ligands allowing the coordination of metal ions at their periphery [18]. Some of the obtained complexes found relevant applications in the field of PDT [19]. For example, porphyrins functionalized with peripheral platinum(II) or ruthenium(II) complexes were used for dual chemo- and phototherapy [20–32]. Platinum(II) complexes have anticancer activity and also, significantly improve the photodynamic effect by promoting the generation of $^1O_2$ through a heavy atom effect [20–28]. Ruthenium(II) complexes were also reported for dual chemo- and phototherapy [29–32]. Moreover, some ruthenium(II) complexes proved to be efficient PS for two-photon excitation [33–35]. Although gold(I) complexes are promising candidates to develop new metallodrugs for cancer therapy, examples of porphyrinoids bearing peripheral gold(I) complexes for combined chemo- and phototherapy are relatively scarce. Gold(I) complexes of porphyrins functionalized with peripheral phosphine ligands were synthesized and biological studies showed that these compounds present rather low cytotoxicity [36]. However, water-soluble complexes of this type proved to be efficient PS for PDT. N-heterocyclic carbenes (NHC) are phosphine analogs and are attractive ligands to design new metallodrugs. During the last decade, we reported the synthesis of several porphyrin derivatives equipped with peripheral NHC-metal complexes [37–41], including gold(I) complexes [42–45]. The photodynamic properties of imidazolium salt **A** and gold(I) complexes **B–D** depicted in Scheme 1 were investigated and we observed the important role played by the ligand *trans* to the NHC [45]. Indeed, the excellent photodynamic properties observed for the PS **D** functionalized with mannose are due to active targeting of cancer cells overexpressing mannose receptors at their surface. We also observed that imidazolium salt **A** is an efficient PS for PDT, while gold(I) complex **B** and **C** are inefficient for chemo- and phototherapy. The aim of this study is to draw more detailed conclusions about the potential of porphyrins equipped with peripheral NHC-gold(I) complexes for dual chemo- and phototherapy. For this purpose, we report here the synthesis and the biological properties of porphyrins bearing imidazolium salts and NHC-gold(I) complexes at their periphery.

2. Results and discussion

2.1. *Synthesis of porphyrins meso-functionalized with imidazolium salts*

Imidazolium salts are routinely used as NHC precursors. NHC could be generated upon deprotonation of an imidazolium salt with a base and trapped with a metal cation such as Ag^+ or Au^+, for example. We first investigated compounds with imidazolium salts directly N-linked to one *meso* position of a porphyrin core. The first imidazolium salt, namely free-base porphyrin **3**, was obtained in a three-step procedure starting from the porphyrin **1** previously described in [46]. The reaction of porphyrin **1** with imidazole and NaH in DMF (140 °C) afforded porphyrin **2** in 72% yield after column chromatography [46]. Then, demetalation of porphyrin **2** in acidic conditions followed by methylation of the peripheral imidazole group with CH_3I afforded porphyrin **3** in an overall yield of 77% after purification (Scheme 2). The ^{1}H NMR spectrum of porphyrin **3** showed the expected signal of the imidazolium proton H^2 at $\delta = 10.44$ ppm and the signal of the two inner NH protons at $\delta = -2.95$ ppm. High-resolution ESI-TOF mass spectrometry (positive mode) featured the expected molecular mass peak at $m/z = 647.2926$ Da

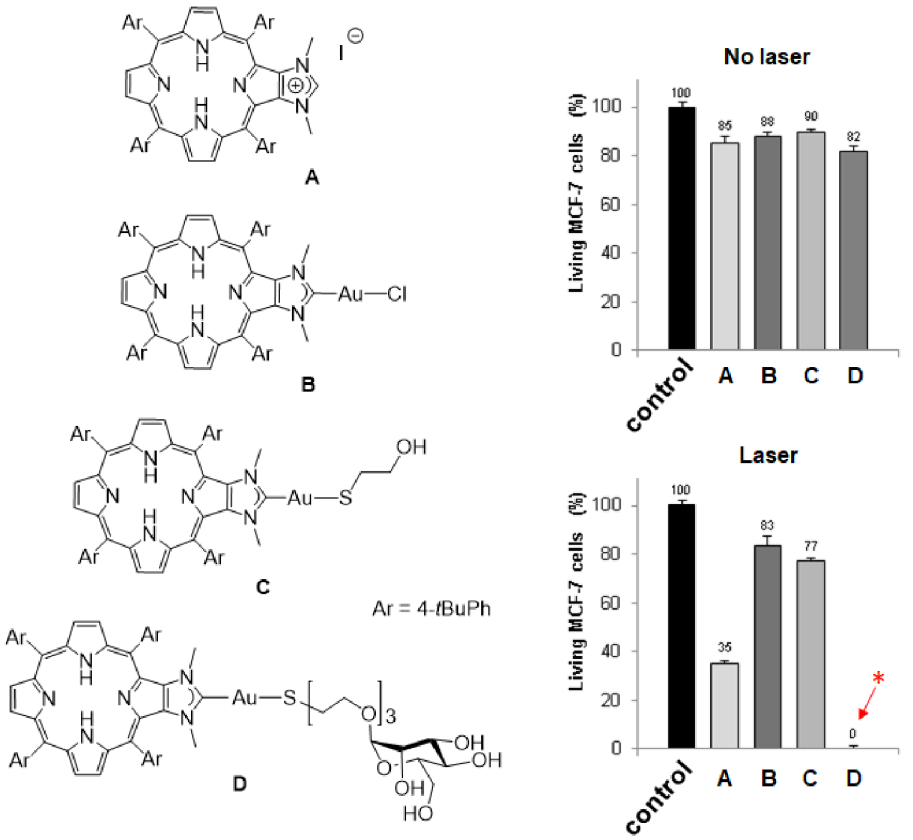

Scheme 1. Left: Structures of compounds **A**–**D**. Right: Cytotoxic (no laser) and photodynamic effect (laser) of imidazolium salt **A** and gold(I) complexes **B**–**D**. The cells were incubated or not (control experiment in black) with 10 µm of PS for 4 h and then, submitted or not to laser irradiation ($\lambda = 405$ nm, 18.75 J·cm^{-2}, 10 min). Cells were allowed to grow for two days and cell viability was quantified with MTT assay. Data are mean values standard deviation from three independent experiments. *No living cells detected [45].

with an isotopically resolved profile in agreement with the calculated distribution for the monocationic species $[M–I]^+$ (calcd $m/z = 647.2918$ Da). The iodide counter-ion was observed by ESI-TOF mass spectrometry (negative mode) at $m/z = 126.91$ Da. Porphyrin **3** was then metalated with $Zn(OAc)_2 \cdot 2H_2O$ to obtain the corresponding zinc(II) porphyrin **4-I** in 80% yield. Metal insertion within the porphyrin core was confirmed by ^{1}H NMR, UV–visible absorption spectroscopy and mass spectrometry (see ESI). To avoid the presence of iodide in the coordination sphere of gold(I) complexes, iodide was substituted by tetrafluoroborate, which is a non-coordinating anion. For this purpose, reaction of porphyrin **4-I** with $AgBF_4$ in acetone in the dark gave porphyrin **4-BF$_4$** in 85% yield after column chromatography. Tetrafluoroborate anion was observed by ^{19}F NMR spectroscopy with the two expected signals at $\delta = -149.20$ and -149.26 ppm (caused by the two boron isotopes ^{10}B and ^{11}B, respectively) and by mass spectrometry (negative mode).

Then, we synthesized imidazolium-based porphyrin compounds with a spacer between the *meso* position of the porphyrin core and the imidazolium salt. For this purpose, free-base porphyrin **5** was used as starting material. The synthesis of this compound is described in [47]. Nucleophilic substitution on the chlorine atom of porphyrin **5** with 1-methylimidazole in DMF (80 °C) afforded porphyrin **6** in 78% yield (Scheme 3). The ^{1}H NMR spectrum

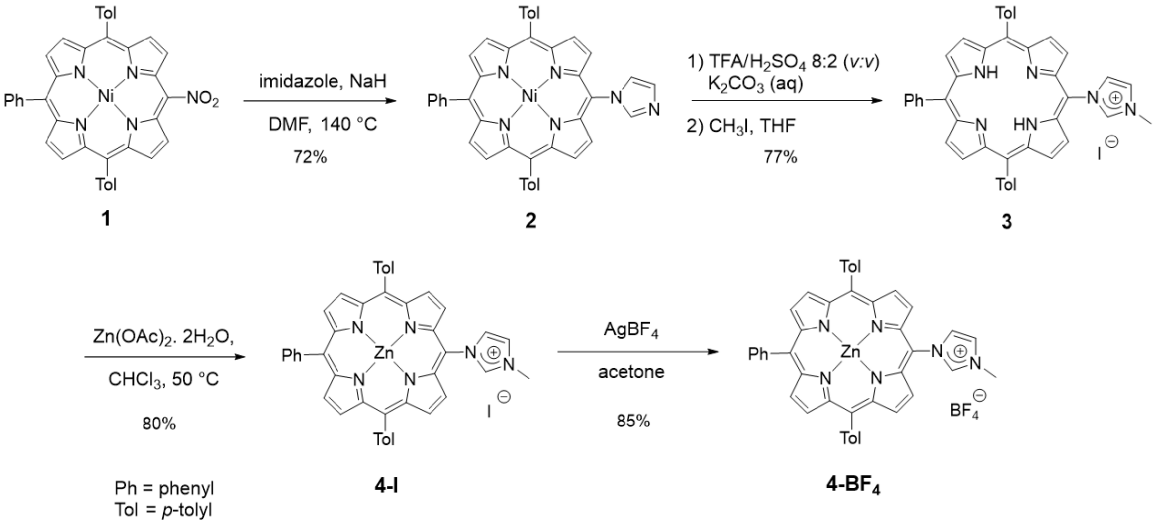

Scheme 2. Synthesis of porphyrins **3**, **4-I** and **4-BF$_4$**.

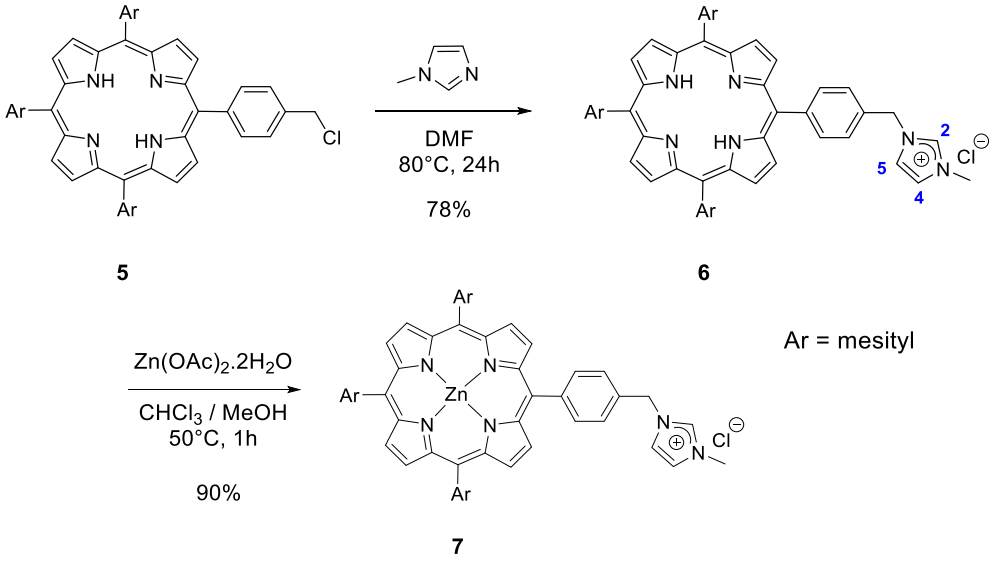

Scheme 3. Synthesis of the porphyrins **6** and **7**.

of the porphyrin **6** clearly showed the expected signal of the imidazolium proton H^2 at δ = 11.17 ppm. The signals of imidazolium protons H^4 and H^5 were also observed as apparent triplets at δ = 7.45 and 7.31 ppm. Porphyrin **7** was obtained in 90% yield by reacting free-base porphyrin **6** with $Zn(OAc)_2 \cdot 2H_2O$.

2.2. *Synthesis of gold(I) complexes*

NHC-gold(I) complexes can be synthesized following different procedures. For example, complex **8** was synthesized in one step by reacting porphyrin **4-BF$_4$** with [AuCl(tht)] (tht = tetrahydrothiophene) in the presence of *t*BuOK in dry THF. The mono(NHC)-gold(I) complex **8** was obtained in 80% yield after column chromatography and recrystallization

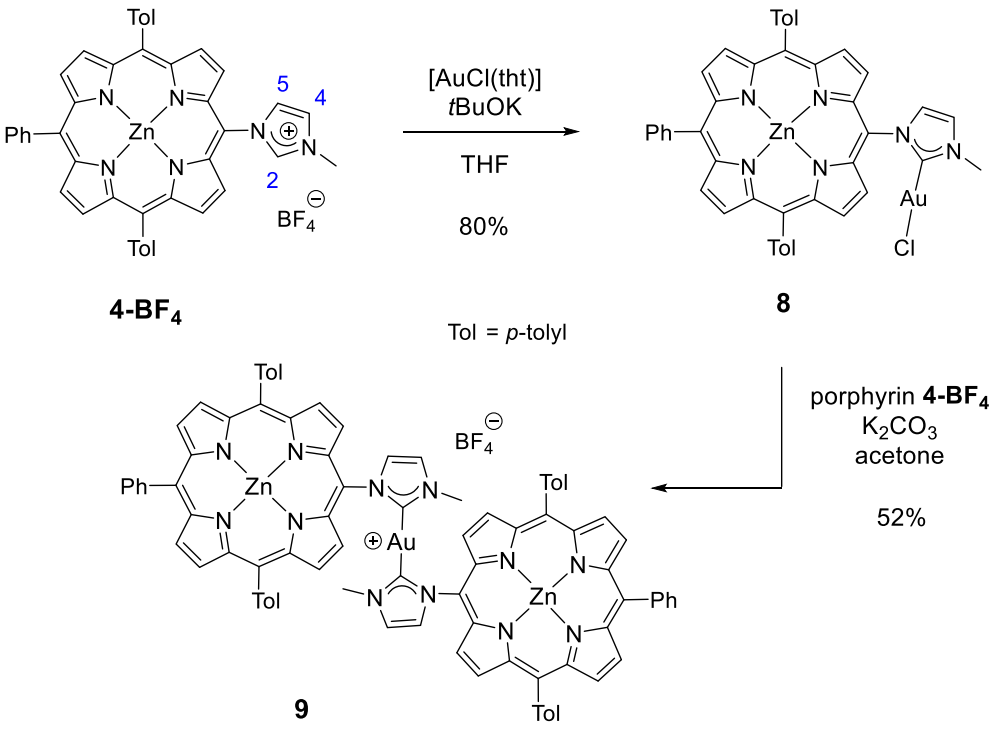

Scheme 4. Synthesis of gold(I) complexes **8** and **9**.

(Scheme 4). The absence of signal corresponding to the imidazolium proton H^2 in the ^{1}H NMR spectrum of complex **8** confirmed the formation of the C_{NHC}–Au(I) bond. Imidazolium protons H^4 and H^5 are shifted upfield by $\Delta\delta \sim 0.40$ ppm as a consequence of the formation of the C_{NHC}–Au(I) bond. The signal of the C_{NHC} bound to Au^I was observed at $\delta = 175.1$ ppm in the $^{13}C\{^1H\}$ NMR spectrum of complex **8**. This chemical shift is in good agreement with those reported in literature for [(NHC)AuCl] complexes [48,49]. Complex **9** was prepared in one step according to the reaction conditions reported by Richeter [42–45]. The deprotonation of the porphyrin **4-BF$_4$** with K_2CO_3 in acetone in the presence of one equivalent of the complex **8** afforded the homoleptic complex **9** in 52% yield after column chromatography (Scheme 4). High-resolution ESI-TOF mass spectrometry (positive mode) featured the expected molecular mass peak at m/z = 1617.3612 Da with an isotopically resolved profile in good agreement with the calculated distribution of the monocationic species $[ZnP–Au–ZnP]^+$ (calcd m/z = 1617.3610 Da). NMR spectroscopy also confirmed the formation of the complex **9**. Notably, in the $^{13}C\{^1H\}$ NMR spectrum, the signal of the C_{NHC} bound to Au^I was observed at $\delta = 188.8$ ppm, a chemical shift in good agreement with those reported in literature for homoleptic monocationic complexes $[(NHC)Au^I(NHC)]^+$ [48,49]. The ^{1}H NMR spectra of complexes **8** and **9** are displayed in Figure 1. Interestingly, in both cases, four separated doublets were observed for the *ortho* and *meta* protons of the tolyl groups. This can be explained by the restricted rotation of the C_{meso}–N_{NHC} bond due to the presence of the sterically demanding NHC-gold(I) complexes. As a consequence, different chemical environments are experienced by the *meso* aryl protons. The N–Me protons signal of complex **9** at $\delta = 2.04$ ppm is significantly shielded ($\delta = 4.23$ ppm for complex **8**) indicating that the N–Me group of one porphyrin sits on top of the second porphyrin ring and is exposed to its ring current. Finally, the two gold(I) complexes were characterized by diffusion-ordered spectroscopy (DOSY) ^{1}H NMR. As expected, the diffusion coefficient of **9** (1.15×10^{-10} $m^2 \cdot s^{-1}$) is lower compared to **8** (1.54×10^{-10} $m^2 \cdot s^{-1}$) because it contains two porphyrins.

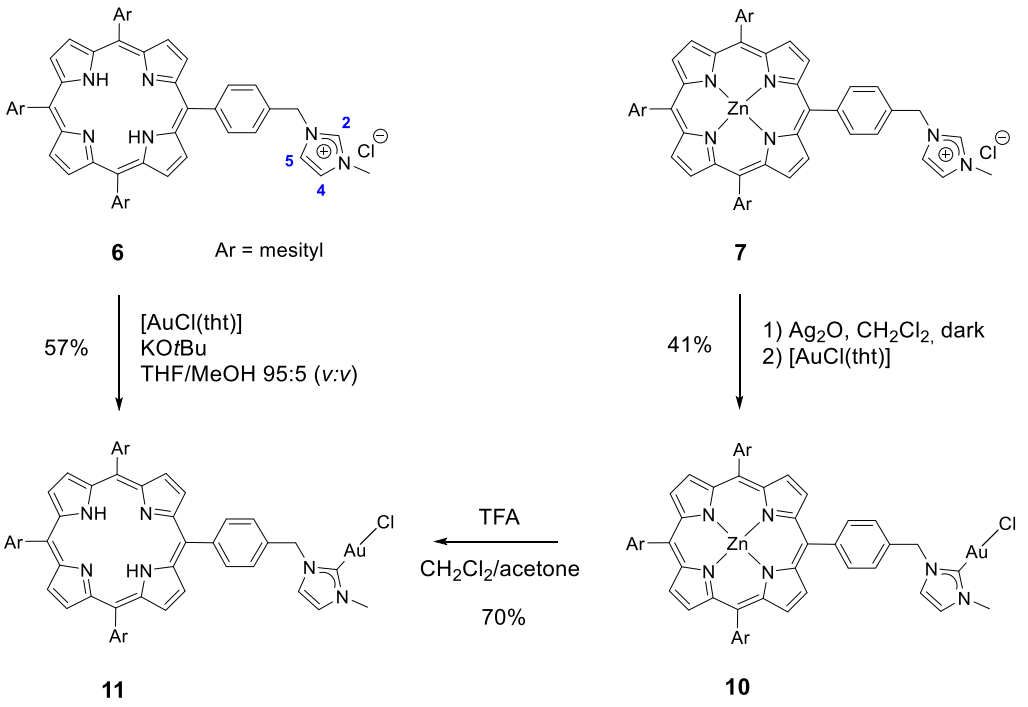

Scheme 5. Synthesis of gold(I) complexes **10** and **11**.

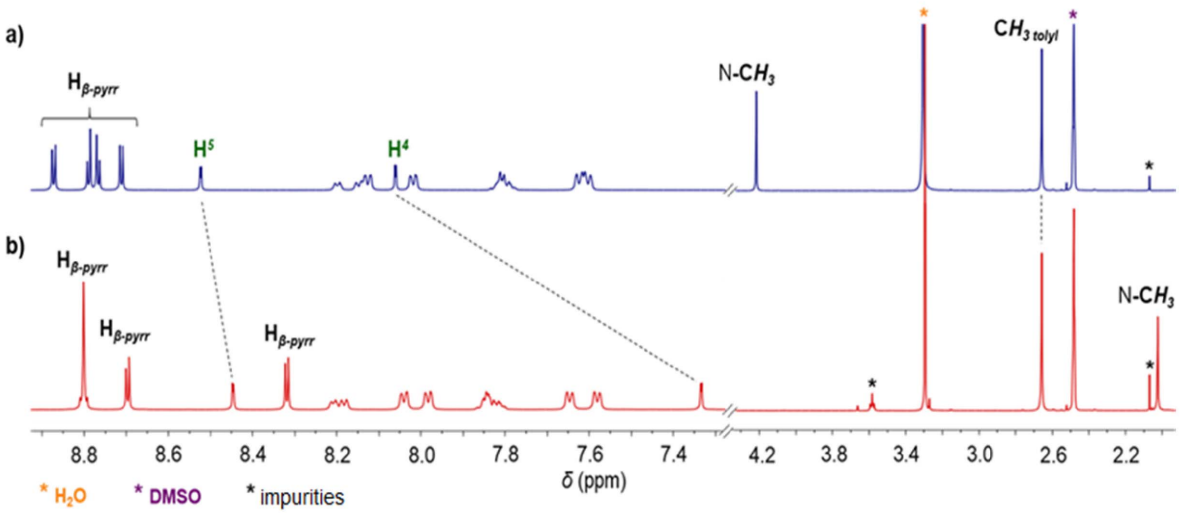

Figure 1. ^{1}H NMR spectra (400 MHz, DMSO-d_6, 298 K) of gold(I) complexes **8** (a) and **9** (b).

Gold(I) complex **10** was prepared following a strategy that is widely used for the synthesis of NHC gold(I) complexes: the reaction of the porphyrin **7** with 1 equation of Ag_2O in dichloromethane afforded the corresponding silver(I) complex which was not isolated and used straightforward for the transmetallation reaction with [AuCl(tht)]. The corresponding gold(I) complex **10** was obtained in 41% yield after column chromatography and recrystallization (Scheme 5). The absence of signal for proton H^2 in

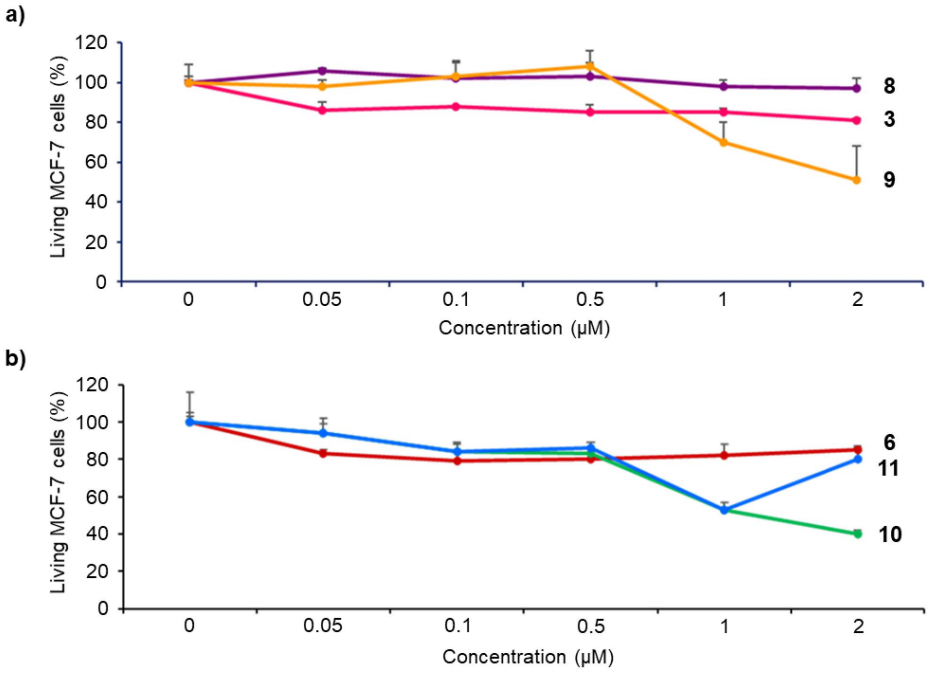

Figure 2. Cytotoxicity of imidazolium salts **3** and **6**, and their corresponding gold(I) complexes **8**–**11** on MCF-7 cancer cells. The cells were incubated without (control) or with 0.05, 0.1, 0.5, 1 or 2 μM of the different compounds for 72 h. Cell viability was quantified with MTT assay. Data are mean values standard deviation from three independent experiments.

the ^{1}H NMR spectrum of complex **10** and the signal of the C_{NHC} bound to Au^{I} observed by $^{13}C\{^{1}H\}$ NMR spectroscopy at δ = 172.3 ppm confirmed the formation of the expected gold(I) complex. Gold(I) complex **11** containing a free-base porphyrin could not be synthesized following a similar strategy because silver(I) may be complexed by the porphyrin core. However, gold(I) complex **11** could be obtained by two different pathways. First, it is possible to remove the zinc(II) by treating the complex **10** with a TFA/CH_2Cl_2 mixture. These acidic conditions do not degrade the peripheral gold(I) complex as it was previously shown by us with analogous complexes [45]. Complex **11** was obtained in 70% yield after neutralization with $NaHCO_3$ and column chromatography. It is also possible to react free-base porphyrin **6** with one equivalent of [AuCl(tht)] with *t*BuOK, in a THF/MeOH mixture in the dark to obtain the corresponding complex gold(I) complex **11** in 57% yield after column chromatography (Scheme 5). The formation of complex **11** was first confirmed by ^{1}H NMR spectroscopy and the disappearance of the signal at δ = 11.17 ppm corresponding to the imidazolium proton H^2. In its $^{13}C\{^{1}H\}$ NMR spectrum, the carbene signal observed at δ = 172.5 ppm demonstrated the formation of the C_{NHC}–Au(I) bond.

2.3. *Cytotoxicity and phototoxicity studies*

Biological properties of NHC-based gold(I) complexes have been extensively reported in literature [50–62]. The cytotoxicity of imidazolium salts and gold(I) complexes on MCF-7 breast cancer cells was first investigated. For this purpose, MCF-7 cancer cells were incubated for 72 h in the dark with each compound at different concentrations varying from 0.05 to 2 μM. After 72 h, MTT assay (3-(4,5-dimethylthiazol-2-yl)-2,5-diphenyltetrazolium bromide) was performed to establish the cell viability and the results obtained are summarized in Figure 2. Free-base porphyrins **3** and **6** containing imidazolium salts are rather non-toxic up to 2 μM with less than 15% cell death irrespective of the presence or not of a linker between the porphyrin core and

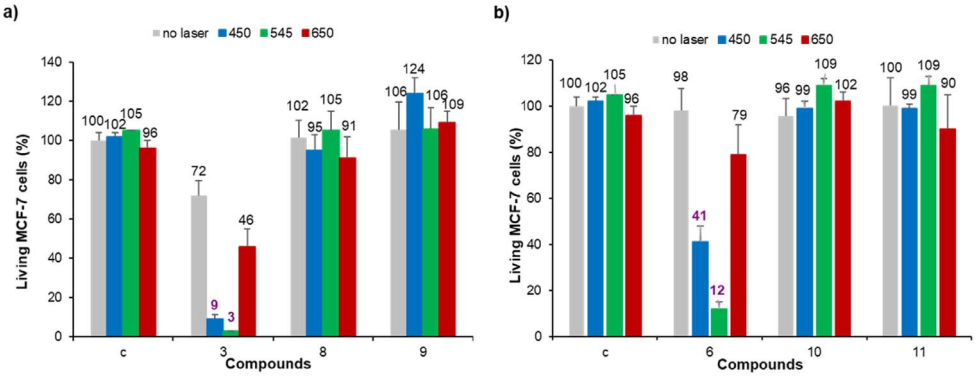

Figure 3. Photodynamic effect of imidazolium salts **3** and **6**, and their corresponding gold(I) complexes **8**-**11** on MCF-7 cancer cells. The cells were incubated with 0.5 μM of each compound for 24 h and then submitted to laser irradiation at λ = 450, 545 or 650 nm for 10 min. Cells are allowed to grow for 48 h and cell viability was quantified with MTT assay.

the NHC. In contrast, gold(I) complexes' cytotoxicity strongly depends on the presence or not of a linker between the porphyrin core and the NHC. Indeed, complex **8** without linker between the porphyrin core and the NHC is not cytotoxic at 2 μM. On the contrary, complex **10** with the *meso*-benzylic linker between the porphyrin core and the NHC shows a significant cytotoxicity with 60% cell death at 2 μM. Therefore, the closer are the porphyrin core and the NHC gold(I) complex, the lower is the observed cytotoxicity. This is in agreement with the low cytotoxicity observed for complex **B** (Scheme 1) where NHC ligand is fused to the porphyrin core. Compound **9** is a cationic bis(NHC) gold(I) complex and it seems that the positive charge tends to increase the observed cytotoxicity since ~50% cell death was observed at 2 μM. Compared to complex **10**, cytotoxicity of the corresponding gold(I) complex **11** including a free-base porphyrin is similar to a concentration up to 1 μM. The lower cytotoxicity observed for complex **11** at a concentration of 2 μM may be attributed to its low solubility in the cell culture medium.

Photodynamic properties of the different compounds were then investigated at 0.5 μM since no or moderate cytotoxicity was observed at this concentration. MCF-7 cancer cells were incubated with the different PS for 24 h and submitted to laser irradiation at λ = 450, 545 or 650 nm for 10 min. The results obtained after MTT assay to estimate cell viability are gathered in Figure 3. As can be seen in this figure, none of the gold(I) complexes showed significant photodynamic effect whatever the irradiation wavelength. This is in agreement with our previous finding that gold(I) complexes without any specific targeting agent are not suitable PS for PDT, although their $^1O_2$ quantum yields may be improved through heavy atom effect [45]. On the contrary, both imidazolium salts **3** and **6** induced important cell death under laser irradiation at λ = 450 and 545 nm. The best photodynamic effect was observed for imidazolium salt **6** at 0.5 μM which induced ~86% cell death after 10 min of irradiation at λ = 545 nm.[1] The good solubility of imidazolium salts in aqueous media and the fact that these cationic species can strongly interact with the negatively charged cancer cell membranes can explain the observed enhanced photodynamic activity compared to the corresponding gold(I) complex. Nevertheless, photodynamic activity of both imidazolium salts **3** and **6** is weaker under irradiation at λ = 650 nm since less than ~19–26% cell death was observed (see footnote 1). This prompted us to investigate the functionalization of pyropheophorbide *a* with imidazole and imidazolium groups and their use for PDT applications.

[1] The values of photo-induced cell death are related to the non-irradiated cells in the same experiment to fairly describe the PDT efficiency, i.e. the cell death induced by light excitation only.

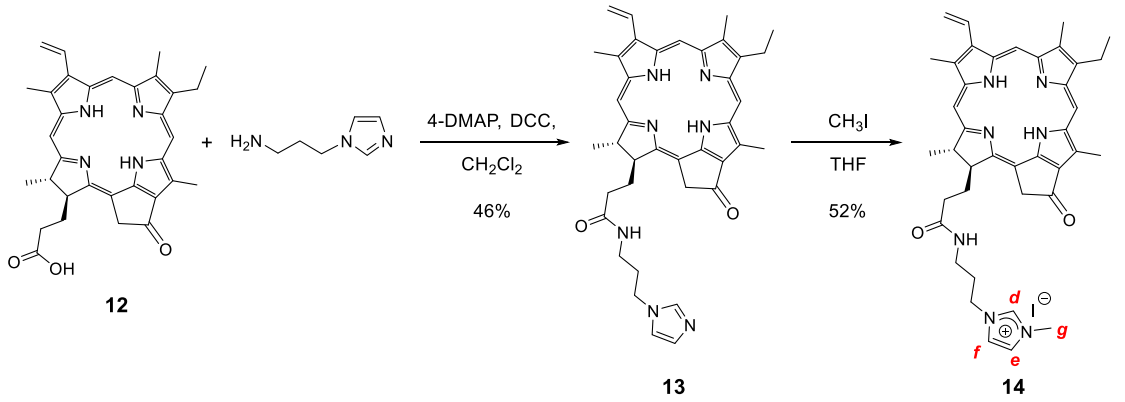

Scheme 6. Synthesis of the monocationic chlorin **14**.

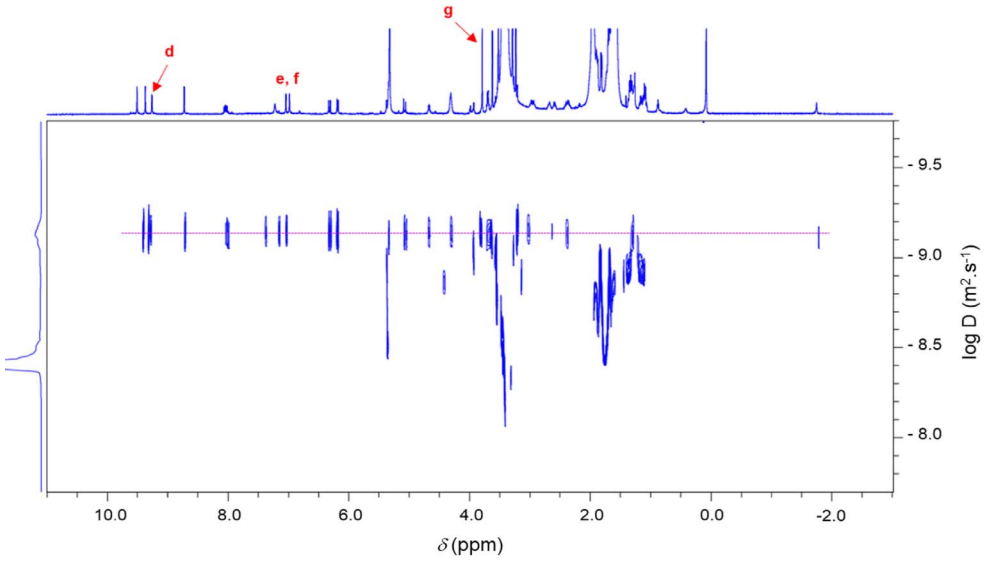

Figure 4. ^{1}H 2D DOSY NMR spectrum (600 MHz, CD_2Cl_2, 298 K) of the chlorin **14**.

2.4. *Synthesis and photodynamic properties of pyropheophorbide a functionalized with imidazole/imidazolium groups*

Monocationic chlorin **14** was prepared in a two-step procedure starting from pyropheophorbide *a* **12** as described in literature (Scheme 6) [63–66]. First, the reaction of pyropheophorbide *a* **12** with 1-(3-aminopropyl)imidazole in the presence of 4-dimethylaminopyridine (DMAP) and dicyclohexylcarbodiimide (DCC) in dry dichloromethane afforded the chlorin **13** in 46% yield [67]. Its ^{1}H NMR spectrum clearly showed three triplets at δ = 7.18, 6.81, and 6.62 ppm corresponding to the protons of the imidazole ring. The signals of the propyl chain were also observed at δ = 3.54 ppm and between 2.90 and 1.90 ppm. Then, methylation of the chlorin **13** with excess of CH_3I in dry THF afforded the monocationic chlorin **14** in 52% yield. Its ^{1}H NMR spectrum clearly showed the deshielded signal of the imidazolium proton at δ = 9.26 ppm. The singlet observed at δ = 3.79 ppm corresponds to the protons of the N–CH_3 group (Scheme 6). In the ^{1}H 2D DOSY NMR spectrum of monocationic chlorin **14**, alignment of the signals of the propyl bearing the imidazolium ring with the other signals of the chlorin core clearly confirmed the formation of the expected compound (Figure 4).

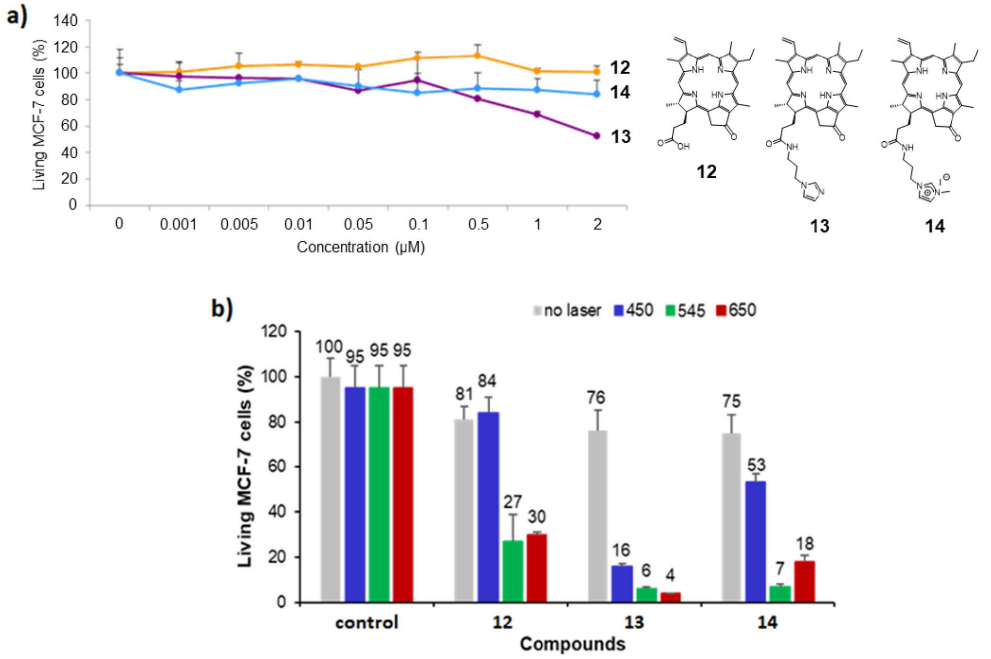

Figure 5. (a) Cytotoxic effect of chlorin derivatives **12**–**14** on MCF-7 cancer cells. The cells were incubated without (control) or with different concentrations of compounds **12**–**14** for 72 h. Cell viability was quantified with MTT assay. Data are mean values standard deviation from three independent experiments. (b) Photodynamic effect of the chlorin derivatives **12**–**14** under irradiation at λ = 450 nm (left), 545 nm (middle) and 650 nm (right). MCF-7 cancer cells were incubated with 0.5 μM of each chlorin for 24 h and then submitted to laser irradiation for 10 min. Cells were allowed to grow for 48 h and the living MCF-7 cells were quantified with MTT assay.

The cytotoxicity studies of chlorin derivatives **12**–**14** on MCF-7 breast cancer cells are summarized in Figure 5a and revealed that pyropheophorbide *a* **12** and imidazolium salt **14** were not cytotoxic on MCF-7 cells because they induce less than 10% cell death at a concentration of 2 μM. On the contrary, imidazole **13** exhibits significant cytotoxicity at 1 μM, with more than 30% cell death (~45% cell death at 2 μM). According to these results, photodynamic activity of chlorin derivatives **12**–**14** was evaluated with PS concentration of 0.5 μM under irradiation at λ = 450, 545 and 650 nm. The obtained data are summarized in Figure 5b. Upon irradiation at λ = 450 nm, only imidazole **13** exhibited a strong photodynamic effect by inducing 60% cell death. Imidazolium salt **14** revealed a slightly phototoxic activity with 22% cell death, whereas pyropheophorbide *a* **12** was not phototoxic at all (Figure 5b, left). Upon irradiation at λ = 545 and 650 nm, all chlorin derivatives **12**–**14** turned out to be phototoxic (Figure 5b, middle and right). The significant phototoxicity of the three chlorins observed upon irradiation at λ = 650 nm constitutes the noteworthy result in this study, since synthetic imidazolium salts **3** and **6** induced less than ~19–26% cell death upon irradiation at λ = 650 nm (Figure 3). Chlorin derivatives **12**, **13** and **14**, induced 51%, 72% and 57% cell death, respectively, and turned out to be better photosensitizers upon irradiation with red light (see footnote 1).

3. Conclusion

Porphyrins bearing imidazolium salts were used as NHC precursors for the synthesis of gold(I) complexes with the aim to combine their cytotoxicity with PDT. This study shows that porphyrins conjugated with NHC-gold(I) complexes are metallodrugs possessing anticancer properties, as long as the NHC ligand is not directly bonded to the porphyrin core: a spacer is probably needed to keep away

the NHC-gold(I) complex from the bulky porphyrin core. Although heavy atom effect may be beneficial to improve $^1O_2$ production, these porphyrins conjugated with gold(I) complexes are not suitable PS for PDT. Additional functionalization with targeting agents is necessary to ensure active targeting of the cancer cells and simultaneously better solubility in aqueous media [68–70]. By contrast, the corresponding porphyrins equipped with imidazolium salt moieties are suitable PS for PDT and this effect is attributed to the positive charges of the imidazolium cations, which are known to ensure strong interactions with negatively charged cancer cell membranes. These cationic porphyrins can induce significant cell death upon laser irradiation at 450 and 545 nm, but not at 650 nm. To improve light absorption and photodynamic effect at 650 nm, pyropheophorbide *a* derivatives equipped with pendant imidazole/imidazolium groups were synthesized. These hemisynthetic compounds proved to be efficient PS for PDT at 650 nm.

4. Experimental section

4.1. *Materials and instruments*

Reactions needing inert atmosphere were performed under argon using oven-dried glassware and Schlenk techniques. Dry THF was obtained by a PureSolve MD5 solvent purification system from Innovative Technology. Dry DMF was purchased from Sigma-Aldrich. Dry CH_2Cl_2 and THF were obtained by a PureSolve MD5 solvent purification system from Innovative Technology. Gold(I) complex [AuCl(tht)] (tht = tetrahydrothiophene) was prepared according to the procedure described in literature [71]. Pyrrole (>99%) was purchased from TCI and distilled under reduced pressure before use. Imidazole (99.5%), iodomethane (99%) and zinc(II) acetate dihydrate (>98%) were purchased from Sigma-Aldrich. Silver tetrafluoroborate (99%) and hydrogen tetrachloroaurate(III) trihydrate ACS 99.99%, Au 49.0% min was used as starting material and purchased from Alfa Aesar. TLC were carried out on Merck DC Kieselgel 60 F-254 aluminum sheets and spots were visualized with UV-lamp (λ = 254/365 nm) if necessary. Preparative purifications were performed by silica gel flash column chromatography (Merck 40–60 μM). NMR spectroscopy and MS spectrometry were performed at the Laboratoire de Mesures Physiques (LMP) of the University of Montpellier (UM). NMR spectra were recorded on Bruker 400 MHz Avance III HD or 600 MHz Avance III spectrometers at 298K. DMSO-d_6, CD_2Cl_2 and CD_3OD were used as received (purchased from Eurisotop, France). ^{1}H and $^{13}C\{^1H\}$ NMR spectra were calibrated to TMS on the basis of the relative chemical shift of the residual non-deuterated solvent as an internal standard. Chemical shifts (δ) are expressed in ppm from the residual non-deuterated solvent signal and coupling constants values (^nJ) are expressed in Hz. Abbreviations used for NMR spectra are as follows: s, singlet; d, doublet; t, triplet; m, multiplet. Mass spectra (HRMS) were recorded on ESI-TOF Q instruments in positive/negative modes. UV–visible absorption spectra were recorded at 25 °C on a JASCO V-650 spectrophotometer in 10 mm quartz cells (Hellma). Molar extinction coefficients ε ($L{\cdot}mol^{-1}{\cdot}cm^{-1}$) are expressed as $\log \varepsilon$.

4.2. *Synthesis and characterization of the different compounds*

4.2.1. *Porphyrin **1***

The synthesis and characterization data of the porphyrin **1** were reported in [46].

4.2.2. *Porphyrin **2***

Porphyrin **1** (150 mg, 0.225 mmol, 1.0 eq) and imidazole (150 mg, 2.25 mmol, 10 eq) were dissolved in dry DMF (11 mL). The solution was purged under Argon atmosphere for 10 min. NaH (60% in suspension in oil, 85 mg, 2.22 mmol, 10 eq) was added and the reaction mixture was stirred at room temperature for 30 min. Then, the reaction mixture was stirred at 140 °C for 1 h. After cooling at room temperature, CH_2Cl_2 (150 mL) was added and the organic phase was washed (distilled H_2O), dried ($MgSO_4$) and concentrated. The residue was purified by column chromatography (SiO_2, eluent from CH_2Cl_2 to CH_2Cl_2/MeOH (98:2)) to give the porphyrin **2** in 72% yield (112 mg). **^{1}H NMR (400 MHz, CD_2Cl_2, 298 K)**: δ 8.86 (d, $^3J_{H–H}$ = 5.0 Hz, 2H, $H_{pyrrole}$), 8.84–8.76 (m 4H, $H_{pyrrole}$), 8.66 (d, $^3J_{H–H}$ = 5.0 Hz, 2H, $H_{pyrrole}$), 8.37 (s, 1H, H^2), 8.05 (s, 1H, H^5), 8.02 (dd, $^3J_{H–H}$ = 7.8 Hz, $^4J_{H–H}$ = 1.6 Hz, H_o), 7.90 (d, $^3J_{H–H}$ = 8.0 Hz, 4H, H_a), 7.79–7.64 (m, 3H, H_m), 7.52 (m, 5H, H_b and H^4), 2.65 (s, 6H, $CH_{3\,tolyl}$). **^{13}C {^{1}H} NMR (150.9 MHz, CD_2Cl_2,**

298, K): δ 144.4, 144.2, 143.7, 142.4, 141.1, 138.5, 137.9, 134.2, 134.2, 134.1 133.2, 133.2, 129.1, 128.7, 128.5, 128.2, 127.5, 121.2, 120.9, 112.8, 21.7 ($CH_{3\,tolyl}$) ppm. **UV–visible (DMSO)**: $\lambda_{max}(\log\varepsilon)$: 414 (5.39), 526 (4.26) nm. **MALDI-TOF$^+$ MS**: calcd for $C_{43}H_{30}N_6Ni$: 689.2, found 689.2.

4.2.3. *Porphyrin **3***

Porphyrin **2** (125 mg, 0.18 mmol, 1.0 eq) was dissolved in a TFA/H_2SO_4 4:1 (v:v) mixture and the reaction was stirred for 45 min at room temperature. Then, the mixture was poured into ice and water and neutralized by K_2CO_3(s). The organic phase was extracted with CH_2Cl_2, dried ($MgSO_4$), and concentrated. The residue was purified by column chromatography (SiO_2, eluent CH_2Cl_2). Recrystallization from CH_2Cl_2/*n*-hexane afforded the free base corresponding porphyrin in 87% yield (100 mg). Then, the obtained compound (90 mg, 0.14 mmol, 1.0 eq) was dissolved in dry THF (25 mL) and CH_3I (2.2 mL, excess) was added. The reaction was stirred at 40 °C for 18 h under argon. Recrystallization from CH_2Cl_2/*n*-hexane afforded the porphyrin **3** as a purple solid in 89% yield (98 mg).

^{1}H NMR (400 MHz, CD_2Cl_2, 298 K): δ 10.44 (t, $^3J_{H–H}$ = 1.7 Hz, 1H, H^2), 9.06–8.98 (m, 5H, $H_{pyrrole}$ and H^5), 8.90–8.86 (m, 4H, $H_{pyrrole}$), 8.40 (t, $^3J_{H–H}$ and $^4J_{H–H}$ = 1.7 Hz, 1H, H^4), 8.24–8.19 (m, 2H, H_o), 8.11 (d, $^3J_{H–H}$ = 7.3 Hz, 4H, H_a), 7.92–7.82 (m, 3H, H_m and H_p), 7.68 (d, $^3J_{H–H}$ = 7.3 Hz, 4H, H_b), 4.31 (s, 3H, N–CH_3), 2.69 (s, 6H, $CH_{3\,tolyl}$), −2.95 (s, 2H, NH) ppm. **^{13}C{^{1}H} NMR (150.9 MHz, DMSO-d_6, 298 K)**: δ 142.5, 140.9, 137.9, 137.5, 134.4, 139.3, 134.3, 134.2, 132.7, 131.9, 130.2, 128.5, 128.2, 128.0, 127.1, 123.3, 123.1, 121.9, 108.7, 36.8 (NCH_3), 21.2 ($CH_{3\,tolyl}$) ppm. **UV–visible (DMSO)**: $\lambda_{max}(\log\varepsilon)$ = 413 (5.32), 525 (4.19), 615 (3.37) nm. **HR ESI-MS (positive mode)**: calcd for $C_{44}H_{35}N_6^+$: 647.2918, found: 647.2926. **ESI-MS (negative mode)**: calcd for I^- 126.91, found: 126.96.

4.2.4. *Porphyrin **4-I***

Porphyrin **3** (50 mg, 0.065 mmol, 1.0 eq) was dissolved in $CHCl_3$(5.5 mL). A solution of $Zn(OAc)_2 \cdot 2H_2O$ (19.8 mg, 0.090 mmol, 1.4 eq) in MeOH (1.5 mL) was added and the reaction was stirred at 50 °C for 1 h. After evaporation of the solvent, recrystallization from CH_2Cl_2/*n*-hexane afforded the porphyrin **4-I** in 80% yield (44 mg). **^{1}H NMR (400 MHz, DMSO-d_6, 298 K)**: δ 10.40–10.36 (br s, 1H, H^2), 8.95 (t, $^3J_{H–H}$ and $^4J_{H–H}$ = 1.8 Hz, 1H, H^5), 8.92 (s, 4H, $H_{pyrrole}$), 8.86–8.78 (m, 4H, $H_{pyrrole}$), 8.38 (t, $^3J_{H–H}$ and $^4J_{H–H}$ = 1.8 Hz, 1H, H^4), 8.22–8.14 (m, 2H, H_o), 8.10–8.02 (m, 4H, H_a), 7.88–7.76 (m, 3H, H_m and H_p), 7.64 (d, $^3J_{H–H}$ = 7.4 Hz, 4H, H_b), 4.30 (s, 3H, N–CH_3), 2.68 (s, 6H, $CH_{3\,tolyl}$) ppm. **^{13}C{^{1}H} NMR (150.9 MHz, DMSO-d_6, 298 K)**: δ 150.6, 150.1, 149.5, 146.9, 142.2, 142.2, 139.1 137.1, 134.3, 134.2, 134.1, 132.7, 133.7, 132.7, 132.3, 130.4, 128.0, 127.9, 127.6, 127.5, 126.8, 123.4, 123.0, 122.2, 108.9, 36.8 (N–CH_3), 21.2 ($CH_{3\,tolyl}$) ppm. **UV–visible (DMSO)**: $\lambda_{max}(\log\varepsilon)$ = 426 (5.37), 516 (3.42), 599 (3.60) nm. **ESI-MS (positive mode)**: calcd for $C_{44}H_{33}N_6Zn^+$: 709.21, found: 709.28. **ESI-MS (negative mode)**: calcd for I^-: 126.91, found: 126.96.

4.2.5. *Porphyrin **4-BF$_4$***

Porphyrin **4-I** (160 mg, 0.19 mmol, 1.0 eq) was dissolved in acetone (50 mL). Then, a solution of $AgBF_4$ (39.5 mg, 0.20 mmol, 1.1 eq) in acetone (2.5 mL) was added dropwise and the reaction mixture was stirred for 1 h under argon at room temperature in the dark. After evaporation, the crude product was purified by column chromatography (SiO_2, eluent from CH_2Cl_2 to CH_2Cl_2/MeOH 95:5, (v:v)). Recrystallization from CH_2Cl_2/*n*-hexane afforded the porphyrin **4-BF$_4$** in 85% yield (125 mg). **^{1}H NMR (400 MHz, DMSO-d_6, 298 K)**: δ 10.39 (br dd, 1H, H^2), 8.95 (t, $^3J_{H–H}$ and $^4J_{H–H}$ = 1.8 Hz, 1H, H^5), 8.91 (s, 4H, $H_{pyrrole}$), 8.84–8.76 (m, 4H, $H_{pyrrole}$), 8.37 (t, $^3J_{H–H}$ and $^4J_{H–H}$ = 1.8 Hz, 1H, H^4), 8.21–8.15 (m, 2H, H_o), 8.08–8.03 (m, 4H, H_a), 7.83–7.79 (m, 3H, H_m and H_p), 7.63 (d, $^3J_{H–H}$ = 7.4 Hz, 4H, H_b), 4.30 (s, 3H, N–CH_3), 2.68 (s, 6H, $CH_{3\,tolyl}$) ppm. **^{13}C{^{1}H} NMR (150.9 MHz, DMSO-d_6, 298 K)**: δ 150.6, 150.1, 149.5, 146.9, 142.2, 142.2, 139.1 137.1, 134.3, 134.2, 134.1, 132.7, 133.7, 132.7, 132.3, 130.4, 128.0, 127.9, 127.6, 127.5, 126.8, 123.4, 123.0, 122.2, 108.9, 36.8 (N–CH_3), 21.2 ($CH_{3\,tolyl}$) ppm. **^{19}F (400 MHz, DMSO-d_6, 298 K)**: δ −149.26 (s), −149.20 (s) ppm. **UV–visible (CH_2Cl_2)**: $\lambda_{max}(\log\varepsilon)$ = 420 (5.79), 518 (3.18), 548 (4.40) nm. **ESI-MS (positive mode)**: calcd for $C_{44}H_{33}N_6Zn^+$: 709.21, found: 709.28. **ESI-MS (negative mode)**: calcd for BF_4^-: 87.00, found: 86.98.

4.2.6. *Porphyrin **5***

The synthesis and characterization data of the porphyrin **5** were reported in [47].

4.2.7. *Porphyrin* ***6***

Porphyrin **5** (160 mg, 0.2 mmol, 1.0 eq) was dissolved in dry DMF (15 mL) and 1-methylimidazole (1.1 mL, 100 eq) was added. The solution was stirred at 80 °C for 24 h under argon atmosphere. Alkylation completion was monitored by TLC. Once finished, the solvent was evaporated under reduced pressure. Recrystallization from CH_2Cl_2/*n*-hexane gave the porphyrin **6** in 78% yield (138 mg). **^{1}H NMR (400 MHz, CD_2Cl_2, 298 K)**: δ 11.17 (br s, 1H, H^2), 8.76 (d, $^3J_{H–H}$ = 4.8 Hz, 2H, $H_{pyrrole}$), 8.67 (d, $^3J_{H–H}$ = 4.8 Hz, 2H, $H_{pyrrole}$), 8.63 (br s, 4H, $H_{pyrrole}$), 8.28 (d, $^3J_{H–H}$ = 8.0 Hz, 2H, H_o), 7.86 (d, $^3J_{H–H}$ = 8.0 Hz, 2H, H_m), 7.45 (t, $^3J_{H–H}$ and $^4J_{H–H}$ = 1.8 Hz, 1H, H^5), 7.31 (dd, $^3J_{H–H}$ and $^4J_{H–H}$ = 1.8 Hz, 1H, H^4), 7.29 (broad s, 6H, $H_{mes\,meta}$), 5.94 (s, 2H, CH_2), 4.16 (s, 3H, N–CH_3), 2.61 (s, 9H, $CH_{3\,mes\,para}$), 1.83–1.86 (2s, 18H, $CH_{3\,mes\,ortho}$), −2.62 (s, 2H, NH) ppm. **^{13}C{^{1}H} NMR (150.9 MHz, CD_2Cl_2, 298 K)**: δ 143.9, 139.9, 139.8, 138.7, 138.6, 138.5, 135.8, 133.3, 128.3, 127.9, 123.9, 122.4, 121.0, 118.6, 118.6, 118.4, 22.0, 21.9, 21.7 ppm. **UV–visible (CH_2Cl_2)**: $\lambda_{max}(\log\varepsilon)$ = 418 (5.41), 515 (4.05), 548 (3.55), 590 (3.52), 648 (3.31) nm. **HR ESI-MS (positive mode)**: calcd for $C_{58}H_{55}N_6^+$: 835.4488, found: 835.4494.

4.2.8. *Porphyrin* ***7***

Porphyrin **6** (110 mg, 0.126 mmol, 1.0 eq) was dissolved in $CHCl_3$ (12 mL). A solution of $Zn(OAc)_2 \cdot 2H_2O$ (41.6 mg, 0.189 mmol, 1.5 eq) in MeOH (2.6 mL) was added and the solution was stirred at 50 °C for 1 h. Then, the solvent was evaporated under reduced pressure. Recrystallization from CH_2Cl_2/*n*-hexane afforded the porphyrin **7** in 90% yield (106 mg). **^{1}H NMR (400 MHz, DMSO-d_6, 298 K)**: δ 9.46 (t, $^4J_{H–H}$ = 1.7 Hz, 1H, H^2), 8.64 (d, $^3J_{H–H}$ = 4.6 Hz, 2H, $H_{pyrrole}$), 8.56 (d, $^3J_{H–H}$ = 4.6 Hz, 2H, $H_{pyrrole}$), 8.54–8.50 (m, 4H, $H_{pyrrole}$), 8.22 (d, $^3J_{H–H}$ = 8.1 Hz, 2H, H_o), 8.07 (t, $^3J_{H–H}$ and $^4J_{H–H}$ = 1.7 Hz, 1H, H^5), 7.87 (t, $^3J_{H–H}$ and $^4J_{H–H}$ = 1.7 Hz, 1H, H^4), 7.77 (d, $^3J_{H–H}$ = 8.1 Hz, 2H, H_m), 7.30 (broad s, 6H, $H_{mes\,meta}$), 5.78 (s, 2H, CH_2), 3.98 (s, 3H, N–CH_3), 2.57 (s, 9H, $CH_{3\,mes\,para}$), 1.78, 1.77, 1.75 (3s, 18H, $CH_{3\,mes\,ortho}$) ppm. **^{13}C{^{1}H} NMR (150.9 MHz, DMSO-d_6, 298 K)**: δ 149.0, 149.0, 148.9, 148.8, 143.2, 139.1, 139.0, 138.4, 138.4, 137.1, 136.9, 136.8, 134.6, 133.9, 131.5, 130.5, 130.0, 127.6, 126.2, 124.2, 122.8, 118.4, 117.7, 51.9, (–CH_2), 36.0 (N–CH_3), 21.6, 21.5, 21.0 ($CH_{3\,ortho}$, $CH_{3\,para}$) ppm. **UV–visible (CH_2Cl_2)**: $\lambda_{max}(\log\varepsilon)$ = 420 (5.63), 549 (4.22) nm. **HR ESI-MS (positive mode):** calcd for $C_{58}H_{53}N_6Zn^+$: 897.3623, found: 897.3632.

4.2.9. *Gold(I) complex* ***8***

Porphyrin **4-BF_4** (60 mg, 0.075 mmol, 1.0 eq) and [AuCl(tht)] (26.5 mg, 0.083 mmol, 1.1 eq) were dissolved in dry THF (6.3 mL). A solution of *t*BuOK (9.3 mg, 0.083 mmol, 1.1 eq) in THF/MeOH (2.3 mL/10 drops) was added dropwise and the reaction mixture was stirred at room temperature under argon for 18 h. After evaporation, the crude was purified by column chromatography (SiO_2, eluent CH_2Cl_2). Recrystallization from CH_2Cl_2/*n*-hexane gave the gold(I) complex **8** as a dark pink solid in 80% yield (72 mg).

^{1}H NMR (600 MHz, DMSO-d_6, 298 K): δ 8.87 (d, $^3J_{H–H}$ = 4.6 Hz, 2H, $H_{pyrrole}$), 8.80–8.76 (m, 4H, $H_{pyrrole}$), 8.71 (d, $^3J_{H–H}$ = 4.6 Hz, 2H, $H_{pyrrole}$), 8.52 (d, $^3J_{H–H}$ = 1.9 Hz, 1H, H^5), 8.21–8.11 (m, 4H, H_o), 8.06 (d, $^3J_{H–H}$ = 1.9 Hz, 1H, H^4), 8.02 (dd, $^3J_{H–H}$ = 7.3 Hz and $^4J_{H–H}$ = 2.1 Hz, 2H, H_a) 7.82–7.78 (m, 3H, H_m and H_p), 7.64–7.58 (m, 4H, H_b), 4.23 (s, 3H, N–CH_3), 2.67 (s, 6H, $CH_{3\,tolyl}$) ppm. **^{13}C{^{1}H} NMR (150.9 MHz, DMSO-d_6, 298 K)**: δ 175.1 (C_{NHC}), 150.2, 150.0, 149.3, 148.1, 142.4, 139.3,136.9, 134.15, 134.1, 134.0,133.0, 132.1, 131.9, 130.2, 128.4, 127.3, 126.6, 122.4, 121.5, 121.2, 113.7, 38.1 ($CH_{3\,tolyl}$), 21.1 (N–CH_3) ppm. **^{1}H DOSY NMR (600 MHz, CD_2Cl_2, 298 K)**: 1.54×10^{-10} $m^2 \cdot s^{-1}$. **UV–visible (CH_2Cl_2)**: $\lambda_{max}(\log\varepsilon)$ = 420 (5.75), 548 (4.38) nm. **HR ESI-MS (positive mode)**: calcd for $C_{44}H_{32}AuClN_6Zn$: 946.1911, found: 946.1923.

4.2.10. *Gold(I) complex* ***9***

Complex **8** (45 mg, 0.048 mmol, 1.0 eq) and porphyrin **4-BF_4** (34.6 mg, 0.044 mmol, 0.90 eq) were dissolved in acetone/MeOH (18 mL/0.5 mL). Then, K_2CO_3 (6.7 mg, 0.048 mmol, 1.0 eq) was added and the reaction mixture was stirred at room temperature for 16 h under argon in the dark. After evaporation, the crude was purified by column chromatography (SiO_2, eluent from CH_2Cl_2 to CH_2Cl_2/MeOH 95:5 (v:v)). Recrystallization from CH_2Cl_2/*n*-hexane afforded the gold(I) complex **9** in 52% yield (40 mg).

^{1}H NMR (600 MHz, DMSO-d_6, 298 K): δ 8.80 (s, 8H, $H_{pyrrole}$), 8.70 (d, 4H, $^3J_{H–H}$ = 4.5 Hz, $H_{pyrrole}$), 8.45 (d, $^3J_{H–H}$ = 1.8 Hz, 2H, H^5), 8.32 (d,

$^3J_{H–H}$ = 4.5 Hz, 4H, $H_{pyrrole}$), 8.22–8.17 (m, 4H, H_o), 8.04 and 7.98 (2dd AB system, $^3J_{H–H}$ = 7.7 and 2.0 Hz, each 4H, H_a), 7.89–7.79 (m, 6H, H_m and H_p), 7.65 and 7.58 (2dd AB system, $^3J_{H–H}$ = 7.7 and 2.0 Hz, each 4H, H_b), 7.34 (d, $^3J_{H–H}$ = 1.8 Hz, 2H, H^4), 2.68 (s, 12H, $CH_{3\,tolyl}$), 2.04 (s, 6H, N–CH_3) ppm. **$^{13}C\{^1H\}$ NMR (150.9 MHz, DMSO-d_6, 298 K)**: δ 188.8 (C_{NHC}), 150.2, 150.0, 149.8, 149.5, 147.6,142.3, 139.2,136.9, 134.1, 134.0, 133.9,132.7, 132.3, 132.0, 129.7, 128.3, 127.7, 127.4, 126.7, 122.4, 121.5, 113.6, 35.1 ($CH_{3\,tolyl}$), 21.0 (N–CH_3) ppm. **^1H DOSY NMR (600 MHz, CD_2Cl_2, 298 K)**: 1.15 × $10^{-10}m^2{\cdot}s^{-1}$. **UV–visible (CH_2Cl_2)**: $\lambda_{max}(\log\varepsilon)$ = 420 (5.75), 548 (4.38) nm. **High-resolution ESI-MS (positive mode)**: calcd for $C_{88}H_{32}Au_2N_{12}Zn_2^+$: 1617.3610, found: 1617.3612. **HR ESI-MS (negative mode)**: calcd for BF_4^-: 87.00, found: 86.98.

4.2.11. *Gold(I) complex **10***

Porphyrin **7** (40 mg, 0.043 mmol, 1.0 eq) was dissolved in dry CH_2Cl_2 (10 mL). Then, Ag_2O (9.9 mg, 0.043 mmol, 1.0 eq) was added and the reaction mixture was vigorously stirred at room temperature under argon protected from light. After 16 h, [AuCl(tht)] (13.7 mg, 0.043 mmol, 1.0 eq) was added and the mixture was stirred for 18 h under the same conditions. The solvent was evaporated under reduced pressure and the crude compound was purified by column chromatography (SiO_2, eluent CH_2Cl_2). Recrystallization from CH_2Cl_2/*n*-hexane gave the gold(I) complex **10** as a red-purple solid in 41% yield (20 mg). **^1H NMR (400 MHz, CD_2Cl_2, 298 K)**: δ 8.84 (d, $^3J_{H–H}$ = 4.6 Hz, 2H, $H_{pyrrole}$), 8.73 (d, $^3J_{H–H}$ = 4.6 Hz, 2H, $H_{pyrrole}$), 8.69 (d, $^3J_{H–H}$ = 1.2 Hz, 4H, $H_{pyrrole}$), 8.23 (d, $^3J_{H–H}$ = 8.0 Hz, 2H, H_o), 7.69 (d,$^3J_{H–H}$ = 8.0 Hz, 2H, H_m), 7.29 (broad s, 6H, $H_{mes\,meta}$), 7.26 (d, $^3J_{H–H}$ = 2.0 Hz, 1H, H^5), 7.13 (d, $^3J_{H–H}$ = 2.0 Hz, 1H, H^4), 5.74 (s, 2H, CH_2), 3.96 (s, 3H, N–CH_3), 2.62 (s, 9H, $CH_{3\,mes\,para}$), 1.84–1.82 (2s, 18H, $CH_{3\,mes\,ortho}$) ppm. **^{13}C $\{^1H\}$ NMR (150.9 MHz, CD_2Cl_2, 298 K)**: δ 172.3 (C_{NHC}), 150.4, 150.4, 150.3, 150.2, 143.8, 139.7, 139.6, 139.5, 139.4, 138.1, 135.4, 135.3, 138.4, 135.6, 135.5, 132.4, 131.6, 131.5, 131.1, 128.1, 126.5, 123.2, 121.4, 119.7, 119.4, 119.3, 55.5 (CH_2), 38.9 (N–CH_3), 22.0, 21.9, 21.7 ($CH_{3\,mes\,ortho}$, $CH_{3\,mes\,para}$) ppm. **UV–visible (CH_2Cl_2)**: $\lambda_{max}(\log\varepsilon)$ = 420 (5.75), 549 (4.36) nm. **MALDI-TOF$^+$ MS**: calcd for $C_{64}H_{55}Au_4N_{12}Cl_4$: 1128.29, found 1128.30.

4.2.12. *Gold(I) complex **11***

Procedure A. Porphyrin **6** (40 mg, 0.043 mmol, 1.0 eq) was dissolved in dry THF (10.5 mL). Then, [AuCl(tht)] (15.4 mg, mmol, 1.1 eq) was added and the mixture was degassed with argon for 10 min. *t*BuOK (6 mg, mmol, 1.1 eq) was dissolved in MeOH (0.5 mL) and added dropwise to the reaction mixture, which was stirred at room temperature for 18 h under argon in the dark. Then, the solvent was evaporated under reduced pressure and the residue was purified by column chromatography (SiO_2, eluent CH_2Cl_2). Recrystallization from CH_2Cl_2/*n*-hexane afforded the gold(I) complex **11** as a purple solid in 57% yield (28 mg). *Procedure B.* Porphyrin **10** (30 mg, 0.027 mmol) was dissolved in acetone (12 mL) under argon. Then, a CH_2Cl_2/TFA 4:1 mixture (6 mL) was slowly added and the reaction mixture was stirred for 30 mn. After neutralization with $NaHCO_3$, the solvent was evaporated and the residue purified by column chromatography (SiO_2, eluent CH_2Cl_2). Recrystallization from CH_2Cl_2/*n*-hexane afforded the gold(I) complex **11** as a purple solid in 70% yield (20 mg). **^1H NMR (400 MHz, CD_2Cl_2, 298 K)**: δ 8.77 (d, $^3J_{H–H}$ = 4.8 Hz, 2H, $H_{pyrrole}$), 8.67 (d, $^3J_{H–H}$ = 4.8 Hz, 2H, $H_{pyrrole}$), 8.63 (s, 4H, $H_{pyrrole}$), 8.22 (d, $^3J_{H–H}$ = 8.0 Hz, 2H, H_o), 7.69 (d, $^3J_{H–H}$ = 8.0 Hz, 2H, H_m), 7.29 (s, 6H, $H_{mes\,meta}$), 7.24 (d, $^3J_{H–H}$ = 1.9 Hz, 1H, H^5), 7.12 (d, 1H, $^3J_{H–H}$ = 1.9 Hz, H^4), 5.73 (s, 2H, CH_2), 3.95 (s, 3H, N–CH_3), 2.61 (s, 9H, $CH_{3\,mes\,para}$), 1.86–1.84 (2s, 18H, $CH_{3\,mes\,ortho}$), −2.62 (s, 2H, NH) ppm. **$^{13}C\{^1H\}$ NMR (150.9 MHz, CD_2Cl_2, 298 K)**: δ 172.5 (C_{NHC}), 143.0, 139.9, 138.9, 138.8, 138.6, 138.4, 135.6, 135.5, 128.3, 126.7, 123.2, 121.4, 118.8, 118.6, 118.4, 55.5 (CH_2), 39.0 (N–CH_3), 21.9 (2s, $CH_{3\,mes\,ortho}$), 21.7 ($CH_{3\,mes\,para}$) ppm. **UV–visible (CH_2Cl_2)**: $\lambda_{max}(\log\varepsilon)$ = 418 (5.65), 514 (4.28), 548 (3.80), 590 (3.75), 647 (3.55) nm. **MALDI-TOF$^+$ MS**: calcd for $C_{64}H_{55}Au_4N_{12}Cl_4$: 1066.38, found 1066.40.

4.2.13. *Pyropheophorbide **a** **12***

The synthesis and characterization data of **pyropheophorbide *a* 12** were reported in [63–66].

4.2.14. *Chlorin **13***

Pyropheophorbide *a* **12** (62 mg, 0.12 mmol, 1.0 eq), 1-(3-aminopropyl)imidazole (18.6 µL, 0.16 mmol, 1.4 eq) and 4-DMAP (18.4 mg, 0.15 mmol, 1.3 eq) were dissolved in dry CH_2Cl_2 (4.0 mL). DCC

(31.1 mg, 0.15 mmol, 1.3 eq) was portionwise added at 0 °C under argon atmosphere. The reaction mixture was stirred at room temperature for 3 h in the dark. The reaction was monitored by TLC. Once finished, H_2O (4.0 mL) was added and the mixture was stirred for 15 min. Then, organic phase was extracted with CH_2Cl_2, washed (distilled H_2O), dried ($MgSO_4$) and concentrated. The residue was dissolved in a minimum amount of CH_2Cl_2 and refrigerated overnight. The crude was then filtered, washed with cold CH_2Cl_2, and the filtrate was concentrated (the operation was reiterated twice). Recrystallization from CH_2Cl_2/*n*-hexane afforded the chlorin **13** as a dark green solid in 46% yield (34 mg). **^{1}H NMR (400 MHz, CD_2Cl_2, 298 K)**: δ 9.44, 9.41, 8.64 (each s, each 1H, *5*, *10* and *20*-H), 8.04 (dd, $^3J_{H–H}$ = 17.8, 11.6 Hz, 1H, 3^1), 7.18 (br dd, 1H, H_d), 6.81 (br dd, $^3J_{H–H}$ = 1.3 Hz and $^4J_{H–H}$ = 1.3 Hz, 1H, H_f), 6.62 (br dd, $^3J_{H–H}$ = 1.3 Hz and $^4J_{H–H}$ = 1.3 Hz, 1H, H_e), 6.34–6.16 (m, 2H, 3^2), 5.24 and 5.06 (2d AB system, $^2J_{H–H}$ = 19.8 Hz, each 1H, 13^2), 4.58–4.51, 4.39–4.36 (each m, each 1H, 17 and 18), 3.75–3.69 (m, 2H, 8^1), 3.59–3.49 (m, 2H, H_c), 3.65, 3.43, 3.26 (each s, each 3H, 2^1, 7^1 and 12^1), 2.89–2.72, 2.66–2.42, 2.25–2.17 and 1.95–1.80 (each m, each 2H, 17^1, 17^2, H_a and H_b), 1.81 (d, $^3J_{H–H}$ = 7.3 Hz, 3H, 18^1), 1.67 (t, $^3J_{H–H}$ = 7.6 Hz, 4H, 8^2), −1.79 (s, 2H, NH) ppm. **UV–visible (CH_2Cl_2)**: $\lambda_{max}(\log\varepsilon)$ = 412 (4.57), 508 (3.88), 538 (3.82), 609 (3.75), 667 (4.13) nm. **MALDI-TOF$^+$ MS**: calcd for $C_{39}H_{43}N_7O_2$ 642.35, found 642.30.

4.2.15. *Chlorin **14***

Chlorin **13** (30 mg, 0.047 mmol, 1.0 eq) was dissolved in dry THF (6.0 mL) and CH_3I (290 µL, 4.7 mmol, 100 eq) was added. The solution was stirred at 40 °C for two days under argon atmosphere and protected from light. The reaction was monitored by TLC. After evaporation of the solvent, recrystallization from CH_2Cl_2/*n*-hexane afforded the monocationic chlorin **14** as a black solid in 52% yield (19 mg). **^{1}H NMR (400 MHz, (CD_2Cl_2/CD_3OD 9:1 (v:v), 298 K)**: δ 9.50, 9.37, 8.72 (each s, each 1H, *5*, *10* and *20*-H), 9.26 (br s, 1H, H_d), 8.04 (dd, $^3J_{H–H}$ = 17.9, 11.5 Hz, 1H, 3^1), 7.04, 6.98 (each br s, each 1H, H_e and H_f), 6.31 and 6.18 (2d AB system, $^2J_{H–H}$ = 19.8 Hz, each 1H, 3^2), 5.32 and 5.07 (2 d AB system, $^2J_{H–H}$ = 19.2 Hz, each 1H, 13^2), 4.70–4.64 and 4.33–4.28 (each m, each 1H, 17 and 18), 3.79 (s, 3H, H_g), 3.62 and 3.23 (each s, each 3H), 3.00–2.91 (m, 2H, H_a), 2.71–2.56 and 2.43–2.32 (each m, each 3H, 17^1, 17^2 and H_b), 1.81 (d, $^3J_{H–H}$ = 7.4 Hz, 1H, 18^1), 1.69 (t, $^3J_{H–H}$ = 7.6 Hz, 4H, 8^2), −1.75 (s, 2H, NH) ppm. **^{13}C{^{1}H} NMR (150.9 MHz, (CD_2Cl_2/CD_3OD 9:1 (v:v), 298 K)**: δ 197.1 (C=O), 174.4, 173.1, 161.8, 155.6, 151.1, 149.4, 145.6, 142.1, 138.1, 137.3, 136.7 (2s), 136.1, 132.8, 130.8, 129.6, 128.6, 123.5, 122.9, 122.7, 104.4, 97.1, 94.5, 52.5, 50.5, 49.6, 48.8, 47.7, 37.0, 35.7, 34.4, 33.6, 31.0, 29.9, 26.2, 25.6, 23.5, 19.9, 17.7, 12.5, 12.2, 11.5 ppm. **UV–visible (CH_2Cl_2)**: $\lambda_{max}(\log\varepsilon)$ = 413 (4.67), 509 (3.75), 540 (3.67), 610 (3.61), 668 (4.28) nm. **HR ESI-MS (positive mode)**: calcd for $C_{40}H_{46}N_7O_2^+$ 656.3708 found 656.3694. **HR ESI-MS (negative mode)**: calcd for I^-: 126.9050 found: 126.9046.

4.3. *Biological studies*

Cell culture. Human breast cancer cells (MCF-7) were purchased from ATCC (American Type Culture Collection, Manassas, VA). Cells were cultured in Dulbecco's Modified Eagle's Medium (DMEM-F12) supplemented with 10% fetal bovine serum and 1% penicillin–streptomycin. Cells were allowed to grow in humidified atmosphere at 37 °C under 5% CO_2.

4.3.1. *Cytotoxicity study in the dark*

MCF-7 cells were seeded into 96-well plates at 5000 cells per well in 200 µL culture medium and allowed to grow for 24 h. Increasing concentrations (from 0 to 2 µM) of compounds were incubated in culture medium of MCF-7 cells during 72 h. Then, a MTT assay was performed to evaluate the toxicity. Briefly, cells were incubated for 4 h with 0.5 mg·mL^{-1} of MTT (3-(4,5-dimethylthiazol-2-yl)-2,5-diphenyltetrazolium bromide; Promega) in media. The MTT/media solution was then removed, and the precipitated crystals were dissolved in EtOH/DMSO (1:1). The solution absorbance was read with a microplate reader at 540 nm.

4.3.2. *PDT experiments*

For 450 nm and 545 nm *in vitro* phototoxicity, 1000 cells by well were plated in a 384-well plates, in 50 µL of culture medium. Twelve hours after seeding, compounds were added on cells at a concentration of 0.5 µM for 24 h. After this incubation, cells were submitted (or not) to laser irradiation for 10 min with the Leica DM IRB at 450 nm (4.6 J·cm^{-2}) or 545 nm

(19.5 J·cm^{-2}). The laser beam was focussed by a microscope objective lens (magnification ×4). Two days after irradiation, an MTT assay was performed to measure the cell viability. For 650 nm *in vitro* phototoxicity, 5000 cells by well were plated in a 96-well plates, in 100 µL of culture medium. Twelve hours after seeding, compounds were added on cells at a concentration of 0.5 µM for 24 h. Then, cells were submitted (or not) to laser irradiation with a red laser at 650 nm for 10 min (18.75 J·cm^{-2}). Two days after irradiation, an MTT assay was performed to evaluate the cell viability.

Acknowledgments

The authors are grateful to the University of Montpellier, the CNRS and the French Ministry of Research for financial support. SR is also grateful for financial support from the Région Languedoc-Roussillon (Research Grant Chercheur(se)s d'Avenir – 2015-005984) and the FEDER Program (Fonds Européen de Développement Régional).

Supplementary data

Supporting information for this article is available on the journal's website under https://doi.org/10.5802/crchim.98 or from the author.

References

[1] T. J. Dougherty, C. J. Gomer, B. W. Henderson, G. Jori, D. Kessel, M. Korbelik, J. Moan, Q. Peng, *J. Natl. Cancer Inst.*, 1998, **90**, 889-905.
[2] P. Jichlinski, H.-J. Leisinger, *Urol. Res.*, 2001, **29**, 396-405.
[3] S. B. Brown, E. A. Brown, I. Walker, *Lancet Oncol.*, 2004, **5**, 497-508.
[4] M. Ethirajian, Y. Chen, P. Joshi, R. K. Pandey, *Chem. Soc. Rev.*, 2011, **40**, 340-362.
[5] B. W. Henderson, T. J. Dougherty, *Photochem. Photobiol.*, 1992, **55**, 145-157.
[6] I. J. MacDonald, T. J. Dougherty, *J. Porphyr. Phthalocyanines*, 2001, **5**, 105-129.
[7] D. E. J. G. J. Dolmans, D. Fukumura, R. K. Jain, *Nat. Rev. Cancer*, 2003, **3**, 380-387.
[8] E. Skovsen, J. W. Snyder, J. D. C. Lambert, P. R. Ogilby, *J. Phys. Chem. B*, 2005, **109**, 8570-8573.
[9] A. E. O'Connor, W. M. Gallagher, A. T. Byrne, *Photochem. Photobiol.*, 2009, **85**, 1053-1074.
[10] R. Bonnett, *Chem. Soc. Rev.*, 1995, **24**, 19-33.
[11] E. D. Sternberg, D. Dolphin, C. Brückner, *Tetrahedron*, 1998, **54**, 4151-4202.
[12] M. Ethirajan, N. J. Patel, R. K. Panda, "19 Porphyrin-Based Multifunctional Agents for Tumor-Imaging and Photodynamic Therapy (PDT)", in *Handbook of Porphyrin Science* (K. M. Kadish, K. M. Smith, R. Guilard, eds.), vol. 4, World Scientific, Singapore, 2010, 249-323.
[13] P. M. Antoni, A. Naik, I. Albert, R. Rubbiani, S. Gupta, P. Ruiz-Sanchez, P. Munikorn, J. M. Mateos, V. Luginbuehl, P. Thamyongkit, U. Ziegler, G. Gasser, G. Jeschke, B. Spingler, *Chem. Eur. J.*, 2015, **21**, 1179-1183.
[14] E. Zenkevich, E. Sagun, V. Knyukshto, A. Shulga, A. Mironov, O. Efremova, R. Bonnett, S. P. Songea, M. Kasem, *J. Photochem. Photobiol. B*, 1996, **33**, 171-180.
[15] Z. Chen, W. Lu, C. Garcia-Prieto, P. Huang, *J. Bioenerg. Biomembr.*, 2007, **39**, 267-274.
[16] C. Moylan, E. M. Scanlan, M. O. Senge, *Curr. Med. Chem.*, 2015, **22**, 2238-2348.
[17] S. Singh, A. Aggarwal, N. V. S. D. K. Bhupathiraju, G. Arianna, K. Tiwari, C. M. Drain, *Chem. Rev.*, 2015, **115**, 10261-10306.
[18] S. Richeter, C. Jeandon, J.-P. Gisselbrecht, R. Ruppert, in *Handbook of Porphyrin Science* (K. M. Kadish, K. M. Smith, R. Guilard, eds.), vol. 3, World Scientific, Singapore, 2010, 429-483.
[19] J.-F. Longevial, C. Clément, J. A. Wytko, R. Ruppert, J. Weiss, S. Richeter, *Chem. Eur. J.*, 2018, **24**, 15442-15460.
[20] H. Brunner, K.-M. Schellerer, B. Treittinger, *Inorg. Chim. Acta*, 1997, **264**, 67-79.
[21] C. Lottner, K.-C. Bart, G. Bernhardt, H. Brunner, *J. Med. Chem.*, 2002, **45**, 2064-2078.
[22] H. Brunner, K.-M. Schellerer, *Inorg. Chim. Acta*, 2003, **350**, 39-48.
[23] C. Lottner, R. Knuechel, G. Bernhardt, H. Brunner, *Cancer Lett.*, 2004, **203**, 171-180.
[24] C. Lottner, R. Knuechel, G. Bernhardt, H. Brunner, *Cancer Lett.*, 2004, **2015**, 167-177.
[25] C. Lottner, K.-C. Bart, G. Bernhardt, H. Brunner, *J. Med. Chem.*, 2002, **45**, 2079-2089.
[26] H. Brunner, N. Gruber, *Inorg. Chim. Acta*, 2004, **357**, 4423-4451.
[27] A. Naik, R. Rubbiani, G. Gasser, B. Spingler, *Angew. Chem. Int. Ed.*, 2014, **53**, 6938-6941.
[28] T. T. Tasso, T. M. Tsubone, M. S. Baptista, L. M. Mattiazzi, T. V. Acunha, B. A. Iglesias, *Dalton Trans.*, 2017, **46**, 11037-11045.
[29] J. Onuki, A. V. Ribas, M. H. G. Medeiros, K. Araki, H. E. Toma, L. H. Catalani, P. Di Mascio, *Photochem. Photobiol.*, 1996, **63**, 272-277.
[30] F. Schmitt, P. Govindaswamy, G. Süss-Fink, W. H. Ang, P. J. Dyson, L. Juillerat-Jeanneret, B. Therien, *J. Med. Chem.*, 2008, **51**, 1811-1816.
[31] F. Schmitt, P. P. Govindaswamy, O. Zava, G. Süss-Fink, L. Juillerat-Jeanneret, B. Therien, *J. Biol. Inorg. Chem.*, 2009, **14**, 101-109.
[32] F. Schmitt, N. P. E. Barry, L. Juillerat-Jeanneret, B. Therien, *Bioorg. Med. Chem. Lett.*, 2012, **22**, 178-180.
[33] N. Sheng, D. Liu, J. Wu, B. Gu, Z. Wang, Y. Cui, *Dyes Pigm.*, 2015, **119**, 116-121.
[34] J. X. Zhang, K.-L. Wong, W.-K. Wong, N.-K. Mak, D. W. J. Kwong, H.-L. Tam, *Org. Biomol. Chem.*, 2011, **9**, 6004-6010.
[35] H. Ke, W. Ma, H. Wang, G. Cheng, H. Yuan, W.-K. Wong, D. W. J.

Kwong, H.-L. Tam, K.-W. Cheah, C.-F. Chan, K.-L. Wong, *J. Lumin.*, 2014, **154**, 356-361.
[36] S. Tasan, C. Licona, P.-E. Doulain, C. Michelin, C. P. Gros, P. Le Gendre, P. D. Harvey, C. Paul, C. Gaiddon, E. Bodio, *J. Biol. Inorg. Chem.*, 2015, **20**, 143-154.
[37] S. Richeter, A. Hadj-Aïssa, C. Taffin, A. van der Lee, D. Leclercq, *Chem. Commun.*, 2007, 2148-2150.
[38] J.-F. Lefebvre, M. Lo, D. Leclercq, S. Richeter, *Chem. Commun.*, 2011, **47**, 2976-2978.
[39] J.-F. Lefebvre, M. Lo, J.-P. Gisselbrecht, O. Coulembier, S. Clément, S. Richeter, *Chem. Eur. J.*, 2013, **19**, 15652-15660.
[40] M. Abdelhameed, P.-L. Karsenti, A. Langlois, J.-F. Lefebvre, S. Richeter, R. Ruppert, P. D. Harvey, *Chem. Eur. J.*, 2014, **20**, 12988-13001.
[41] J.-F. Lefebvre, J.-F. Longevial, K. Molvinger, S. Clément, S. Richeter, *C. R. Chim.*, 2016, **19**, 94-102.
[42] J.-F. Longevial, A. Langlois, A. Buisson, C. H. Devillers, S. Clément, A. van der Lee, P. D. Harvey, S. Richeter, *Organometallics*, 2016, **35**, 663-672.
[43] C. Rose, A. Lebrun, S. Clément, S. Richeter, *Chem. Commun.*, 2018, **54**, 9603-9606.
[44] J.-F. Longevial, M. Lo, A. Lebrun, D. Laurencin, S. Clément, S. Richeter, *Dalton Trans.*, 2020, **49**, 7005-7014.
[45] J.-F. Longevial, K. El Cheick, D. Aggad, A. Lebrun, A. van der Lee, F. Tielens, S. Clément, A. Morère, M. Garcia, M. Gary-Bobo, S. Richeter, *Chem. Eur. J.*, 2017, **23**, 14017-14026.
[46] C. H. Devillers, S. Hebié, D. Lucas, H. Cattey, S. Clement, S. Richeter, *J. Org. Chem.*, 2014, **79**, 6424-6434.
[47] J. S. Lindsey, S. Prathapan, T. E. Johnson, R. W. Wagner, *Tetrahedron*, 1994, **50**, 8941-8968.
[48] S. Gaillard, A. M. Z. Slawin, A. T. Bonura, E. D. Stevens, S. P. Nolan, *Organometallics*, 2010, **29**, 394-402.
[49] D. Marchione, M. A. Izquierdo, G. Bistoni, R. W. A. Havenith, A. Macchioni, D. Zuccaccia, F. Tarantelli, L. Belpassi, *Chem. Eur. J.*, 2017, **23**, 2722-2728.
[50] M. Baker, P. J. Barnard, S. J. Berners-Price, S. K. Brayshaw, J. L. Hickey, B. W. Skelton, A. H. White, *Dalton Trans.*, 2006, 3708-3715.
[51] J. L. Hickey, R. A. Ruhayel, P. J. Barnard, M. V. Baker, S. J. Berners-Price, A. Filipovska, *J. Am. Chem. Soc.*, 2008, **130**, 12570-12571.
[52] R. Rubbiani, I. Kitanovic, H. Alborzinia, S. Can, A. Kitanovic, L. A. Onambele, M. Stefanopoulou, Y. Geldmacher, W. S. Sheldrick, G. Wolber, A. Prokop, S. Wolfl, I. Ott, *J. Med. Chem.*, 2010, **53**, 8608-8618.
[53] R. Rubbiani, S. Can, I. Kitanovic, H. Alborzinia, M. Stefanopoulou, M. Kokoschka, S. Monchgesang, W. S. Sheldrick, S. Wolfl, I. Ott, *J. Med. Chem.*, 2011, **54**, 8646-8657.
[54] A. Gautier, F. Cisnetti, *Metallomics*, 2012, **4**, 23-32.
[55] T. Zou, C. T. Lum, S. S.-Y. Chui, C.-M. Che, *Angew. Chem. Int. Ed.*, 2013, **52**, 2930-2933.
[56] R. Rubbiani, E. Schuh, A. Meyer, J. Lemke, J. Wimberg, N. Metzler-Nolte, F. Meyer, F. Mohr, I. Ott, *Med. Chem. Commun.*, 2013, **4**, 942-948.
[57] B. Bertrand, L. Stefan, M. Pirrotta, D. Monchaud, E. Bodio, P. Richard, P. Le Gendre, E. Warmerdam, M. H. de Jager, G. M. Groothuis, M. Picquet, A. Casini, *Inorg. Chem.*, 2014, **53**, 2296-2303.
[58] R. Rubbiani, L. Salassa, A. de Almeida, A. Casini, I. Ott, *Chem. Med. Chem.*, 2014, **9**, 1205-1210.
[59] P. Holenya, S. Can, R. Rubbiani, H. Alborzinia, A. Junger, X. Cheng, I. Ott, S. Wölfl, *Metallomics*, 2014, **6**, 1591-1601.
[60] R. W.-Y. Sun, M. Zhang, D. Li, Z.-F. Zhang, H. Cai, M. Li, Y.-J. Xian, S. W. Ng, A. S.-T. Wong, *Chem. Eur. J.*, 2015, **21**, 18534-18538.
[61] C. Schmidt, B. Karge, R. Misgeld, A. Prokop, R. Franke, M. Brönstrup, I. Ott, *Chem. Eur. J.*, 2017, **23**, 1869-1880.
[62] B. Dominelli, J. D. G. Correia, F. E. Kuehn, *J. Organomet. Chem.*, 2018, **866**, 153-164.
[63] K. M. Smith, D. A. Goff, D. J. Simpson, *J. Am. Chem. Soc.*, 1985, **107**, 4946-4954.
[64] H. Tamiaki, M. Amakawa, Y. Shimono, R. Tanikaga, A. R. Holzwarth, K. Schaffner, *Photochem. Photobiol.*, 1996, **63**, 92-99.
[65] H. Tamiaki, K. Fukai, H. Shimazu, S. Shoji, *Photochem. Photobiol.*, 2014, **90**, 121-128.
[66] M. Chevrier, A. Fattori, L. Lasser, C. Kotras, C. Rose, M. Cangiotti, D. Beljonne, A. Mehdi, M. Surin, R. Lazzaroni, P. Dubois, M. F. Ottaviani, S. Richeter, J. Bouclé, S. Clément, *Molecules*, 2020, **25**, article no. 198.
[67] G.-I. Sengee, N. Badraa, Y. K. Shim, *J. Porphyr. Phthalocyanines*, 2009, **13**, 818-822.
[68] M. V. Baker, P. J. Barnard, S. J. Berners-Price, S. K. Brayshaw, J. L. Hickey, B. W. Skelton, A. H. White, *J. Organomet. Chem.*, 2005, **690**, 5625-5635.
[69] J. Weaver, S. Gaillard, C. Toye, S. Macpherson, S. P. Nolan, A. Riches, *Chem. Eur. J.*, 2011, **17**, 6620-6624.
[70] B. Bertrand, A. de Almeida, E. P. M. van der Burgt, M. Picquet, A. Citta, A. Folda, M. P. Rigobello, P. Le Gendre, E. Bodio, A. Casini, *Eur. J. Inorg. Chem.*, 2014, 4532-4536.
[71] R. Usón, A. Laguna, M. Laguna, D. A. Briggs, H. H. Murray, J. P. Flacker Jr., *Inorg Synth.*, 1989, **26**, 85-91.